

TRABAJO DE FIN DE GRADO

---

# **Metal-Organic Frameworks for Adsorption of Pollutant Molecules in Water**

---

Norberto Medina Rodríguez

Grado en Física

2020-2021

Tutores:

Dra. Verónica Pino Estévez

Dr. Jorge Pasán García

## INDEX

1. ABSTRACT	2
2. INTRODUCTION	4
2.1 Metal-organic frameworks	4
2.2 Structure details of PCN-250 MOFs	8
2.3 MOF synthesis	9
2.4 MOFs for the removal of Emerging Organic Contaminants in water	10
3. OBJECTIVES	11
4. EXPERIMENTAL SECTION	12
4.1 Reagents	12
4.2 Synthesis	13
4.3 Characterization	16
4.4 Analytical performance	20
5. RESULTS AND DISCUSSION	23
5.1 PXRD patterns	23
5.2 Water stability test	26
5.3 IR spectroscopy	27
5.4 Thermal analysis	28
5.5 Gas uptake	30
5.6 Analytical performance	32
6. CONCLUSIONS	34
7. REFERENCES	35

## 1. ABSTRACT

El presente Trabajo de Fin de Grado ha sido realizado dentro del grupo de investigación MAT4LL de la Universidad de La Laguna. Se trata de un equipo multidisciplinar cuya línea principal de trabajo se centra en el diseño de nuevas fases de extracción basadas en diferentes materiales, siendo las redes metal-orgánicas unos de los principales materiales objeto de investigación.

Las redes metal-orgánicas, MOFs (Metal-Organic Frameworks), son unas estructuras cristalinas formadas por la combinación de cationes o clusters metálicos y ligandos orgánicos. Sus propiedades más relevantes incluyen una porosidad uniforme y permanente, unos de los mayores tamaños de poros hallados en compuestos cristalinos, unas altas superficies específicas y unas capacidades de adsorción muy altas. Debido al enorme número de posibles combinaciones de cluster metálico y ligando orgánico y a la posibilidad de llevar a cabo procesos de funcionalización *in situ* o *post* sintéticos, la variedad estructural y funcional de los MOFs es muy amplia.

Al combinar el amplio control sintético de la química orgánica con la diversidad funcional y geométrica de los compuestos inorgánicos, los MOFs pueden ser deliberadamente diseñados para aplicaciones específicas. Estas aplicaciones incluyen almacenamiento de gases, catálisis, almacenamiento de energía, conductividad eléctrica o transporte de medicamentos.

En los últimos años se han convertido en uno de los materiales más prometedores para el tratamiento de aguas residuales, con especial énfasis en la eliminación de contaminantes orgánicos emergentes (EOCs, por sus siglas en inglés). Estos contaminantes provienen de una amplia variedad de fuentes, y en los últimos años se han diversificado enormemente debido al desarrollo de nuevas sustancias y materiales para su aplicación en diversas industrias. Estudios recientes hacen hincapié en la necesidad de desarrollar nuevos métodos de tratamiento de aguas residuales para eliminarlos, al ser perjudiciales para el medio ambiente y la salud. Al ser el agua un recurso básico para la vida y la salud, su tratamiento y reutilización son factores clave para nuestro planeta.

El presente trabajo ha consistido, en primer lugar, en sintetizar y caracterizar tres MOFs diferentes de la familia PCN-250 y, finalmente, llevar a cabo estudios de adsorción de diferentes contaminantes en agua. Los tres MOFs estudiados han sido el PCN-250(Fe), el PCN-250(Fe<sub>2</sub>Co) y el PCN-250(Fe-IM). El primer paso ha consistido en el escalado de

las reacciones de síntesis halladas en la bibliografía, con el objetivo de obtener la cantidad suficiente de material para hacer la caracterización completa y los estudios de extracción. Las técnicas utilizadas en la caracterización han sido: la difracción de rayos X de polvo (PXRD, por sus siglas en inglés), estudios de estabilidad en agua, análisis térmico (termogravimetría y calorimetría diferencial de barrido), espectroscopía infrarroja y fisisorción de gases. Finalmente, el último estudio ha consistido en realizar la prueba de extracción de contaminantes en agua.

La técnica de difracción de rayos X de polvo da información sobre la estructura cristalina que subyace en las diferentes muestras que se han ido sintetizando, por lo que ha sido utilizada para confirmar que dichas muestras se corresponden con el MOF objetivo. También ha sido utilizada para comprobar la estabilidad en agua de los MOFs, ya que comparando los difractogramas anteriores y posteriores a la exposición al agua se puede comprobar si ha habido colapso de la estructura, descomposición o pérdida de cristalinidad. Esta prueba es indispensable para evaluar los MOFs para tratamiento de aguas, ya que muchos MOFs son descartados para este propósito por su inestabilidad en esta. El análisis térmico nos da información sobre la estabilidad térmica de la estructura, que es relevante para muchas de las potenciales aplicaciones de estos materiales. Dadas las características estructurales de la familia PCN-250, se espera de antemano que muestren una alta estabilidad térmica y en agua. La espectroscopía infrarroja ha sido utilizada para comprobar la presencia de determinados grupos funcionales en las estructuras y para comprobar la efectividad de la retirada de moléculas de disolvente de los poros de los materiales. La prueba de fisisorción de gases es una prueba típica para materiales porosos, ya que da información sobre el tamaño, el volumen y la distribución de los poros de los materiales, y usando la teoría BET se puede inferir su superficie específica. Finalmente, la prueba de extracción de contaminantes en agua se ha realizado mediante el método de extracción dispersiva miniaturizada en fase sólida ( $\mu$ -dSPE), utilizando condiciones óptimas con ocho tipos diferentes de contaminantes variados (fenoles, hidrocarburos, medicamentos, cosméticos y bactericidas), para tener una buena idea del potencial de estos MOFs para la descontaminación de aguas.

Los resultados obtenidos de las pruebas enumeradas anteriormente llevan a las siguientes conclusiones. En primer lugar, dada la coincidencia entre los difractogramas de las muestras sintetizadas y las activadas con los simulados, se puede concluir que los tres MOFs han sido sintetizados correctamente. Además, viendo que en las reacciones

escaladas se han obtenido unos rendimientos similares a los de las reacciones de partida, se puede decir que el escalado ha sido asimismo un éxito. También se ha podido comprobar que el proceso de activación no ha comprometido la estructura cristalina y ha conseguido eliminar gran parte de las moléculas de disolvente de los poros de las muestras. Por otro lado, se ha podido confirmar la gran estabilidad de la estructura PCN-250 tanto al agua (por inmersión a pH neutro hasta 7 días) como a la temperatura (hasta 400 °C). Esto es un buen indicio de que la estabilidad de estos MOFs no será un problema en aplicaciones futuras. El valor de área superficial específica obtenido de las isotermas de adsorción-desorción de nitrógeno ha confirmado que el material es bastante poroso. Finalmente, los buenos ratios de extracción obtenidos en la prueba de extracción miniaturizada dispersiva de fase sólida lleva a la conclusión de que el MOF PCN-250(Fe) tiene potencial para la extracción de contaminantes del agua y formará parte de futuros trabajos del grupo de investigación.

## **2. INTRODUCTION**

---

En esta sección se explicará qué son las redes metal-orgánicas, sus principales propiedades y varios aspectos relevantes acerca de ellas. A continuación, se detallan las características estructurales de las redes estudiadas, pertenecientes a la familia PCN-250. Se explicarán también los principales aspectos relativos a la síntesis de estos materiales y finalmente se comentará su uso en el tratamiento de aguas contaminadas.

---

### **2.1. Metal-organic frameworks**

Metal-organic frameworks (MOFs) are crystalline materials formed by the combination of organic linkers (with two or more coordination sites) with metal cations (or metal clusters) through metal-carboxyl bonds. Figure 2.1 shows an example of how building blocks connect to form the MOF structure. Their properties include uniform and permanent porosity, the largest pores known for crystalline compounds, very high sorption capacities and complex sorption behavior (1, 2).

The properties of the MOF are given by its structural components: the metal cluster and the organic linker. The MOF can be deliberately designed with a certain

structure by considering the geometry of the building blocks. In this sense, a rationale design based on reticular chemistry is always advisable. Being a crystalline structure, this analysis and deliberate design as well as the characterization, fall within the scope of crystal engineering (3).

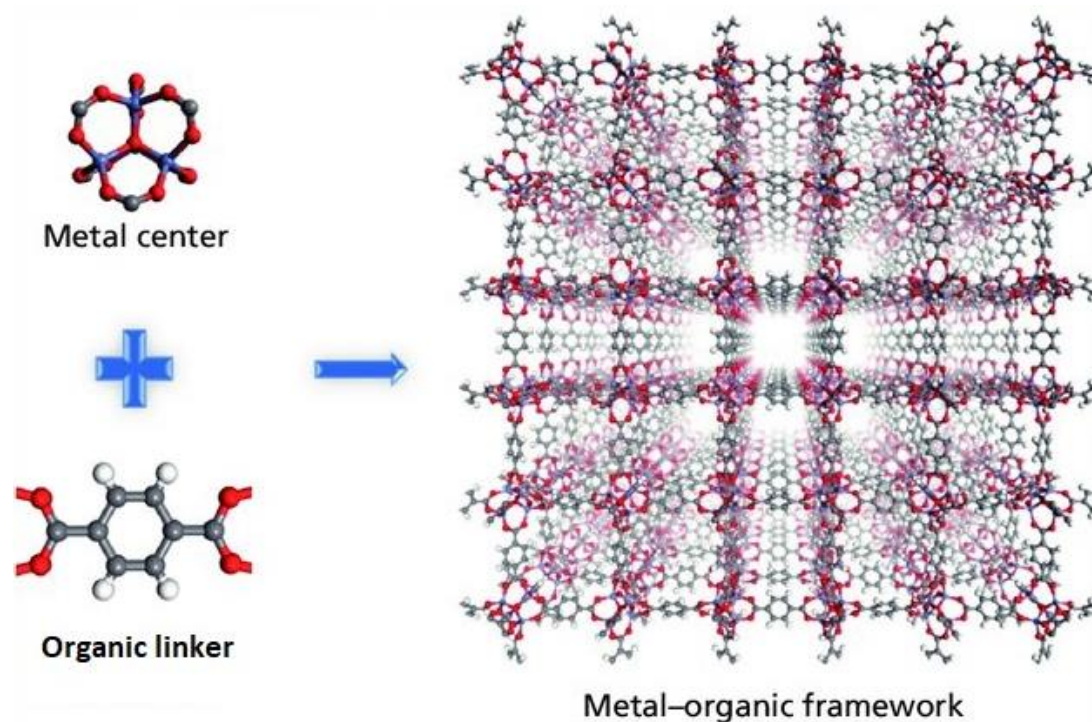


**Figure 2.1.** MOF basic constituents and structure, taken from (4).

The structural classification of said crystal lattice is usually carried out by simplifying the structure in terms of nodes and links. With this description, a framework is invariant to any transformation that does not involve breaking and making connections, such as rotations, translations, distortions, etc. At this point it is necessary to define the “points of extensions”, which is the number of bonds that a building unit makes with other ones. It is said that a building unit (SBU) is  $n$ -connected ( $n$ -c) when it has  $n$  points of extension. Two-connected (2-c) SBUs are considered edges, whereas SBUs with higher connection numbers are considered nodes. Knowing the points of extensions and local symmetry (square, triangle...) of all building units is not always sufficient, sometimes it is necessary to know how they connect with each other and the spatial distribution they take. A net described this way is only unique if it is necessary to break and make its connections to transform it into another. Each unique net is assigned an identifier of three letters (**scu**, **fcu**, ...) (5). Using this description, the structures of the MOFs can be classified and deliberately designed (6, 7, 8).

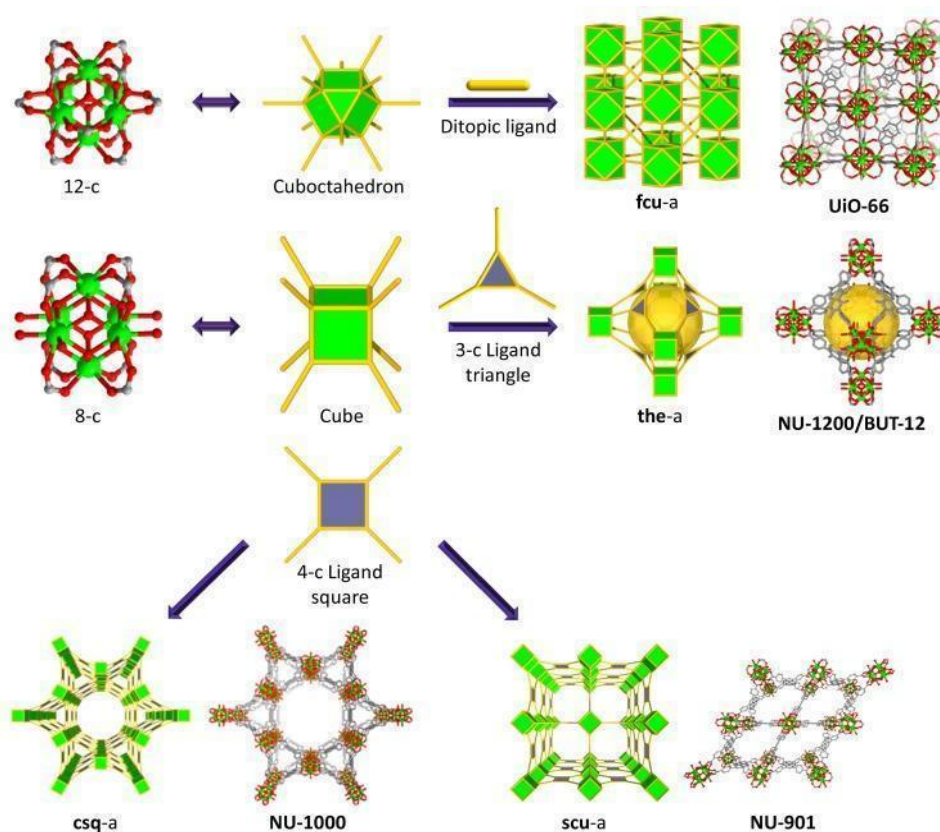


**Figure 2.2.** Examples of different structure topologies depending on the cluster and organic linker geometry and spatial arrangement, taken from (9).

Moreover, MOFs functionalization can be carried out by employing new substituents that bind to the organic linker, and their cluster composition can be changed by using different metals in the synthesis (8). These modifications can alter the MOF adsorption properties. These changes are not always a straightforward process, since the MOF synthesis can be affected by subtle changes in reaction parameters (10). Because of this, post-synthetic modification was developed. These methods allow the successful functionalization of a given MOF without changing their initial structure, porosity, and crystallinity (11, 12, 13).

Due to the large number of possible organic linkers, metal clusters and the possibility of pre- and post-functionalization, MOFs have a wide structural and functional diversity.

Chemical and thermal stability of MOFs is a crucial factor in their analysis, since a structure that easily collapses or decomposes will have little utility when used for various purposes (14). For example, when evaluating a MOF for use in water, it must be verified that it does not decompose in it after a considerable time exposure. Other factors

to consider in this case could be the temperature (15), the pH and the time of exposure to these factors (16).

One way to increase the stability of a MOF is to use polynuclear clusters, commonly referred to as SBUs (Secondary Building Units), instead of simple metal nodes. This is because the chelation of the metal ions when forming these polynuclear clusters provides stronger bonds that translate into rigidity of the structure, while the use of charged linkers favors stronger bonds and the obtention of a neutral framework (8). MOFs built from these principles are very thermally and chemically stable (17). This robustness makes it possible for the structure not to collapse by, for example, removing solvent molecules trapped inside during synthesis.

This process of releasing molecules trapped inside the pores of the material is called "activation". These trapped molecules are basically molecules of the solvent in which the MOF synthesis took place, so removal is usually done by evaporation. This evaporation is carried out through the application of heat and reduced pressure, to remove the molecules evaporated by the heat. In many cases, carrying out this process directly leads to the collapse of the structure, so the first step for the activation of a MOF usually is the exchange of these molecules for others that are easier to eliminate, because they have a lower boiling point, for example. Once this exchange has been carried out, the heat and reduced pressure are applied, thus achieving, in most cases, that the structure does not collapse when the molecules are removed from the pores. With this procedure it is viable to get access to the permanent porosity of the material (8, 16, 18).

This permanent porosity is one of the most interesting properties of MOFs, since this free space can be used for adsorption of other molecules. This adsorption can be used for different purposes, the most common being the storage of gases such as hydrogen and methane (19, 20), catalysis (21, 22), purification and separation of gases (23, 24), electrical conduction (25), energy storage (26) and drug delivery (27). Through isorecticular expansion, systematic variation of the length of the ligands maintaining the same structure, MOFs with pores up to 48 Å in diameter, up to 90% free volume and densities less than 0.13 g/cm<sup>3</sup> have been achieved. Carrying out gas adsorption tests in different MOFs, they show much higher surface area values than other porous materials, such as zeolites and some silicates or carbons, reaching values greater than 7000 m<sup>2</sup>/g (28).



If the structure of a MOF is robust enough, in some cases it is possible to make the adsorption process reversible without structure collapse, thus being able to not only remove the adsorbed molecules from a medium and be able to recover them later, but also to be able to reuse this MOF multiple times (29).

## 2.2. Structural details of PCN-250 MOFs

All the studied MOFs in this work are isostructural variations of the same MOF, the PCN-250. PCN stands for Porous Coordination Network. This MOF is formed by hexagonal clusters ( $D_{3h}$  spatial group) of the form  $M_3O(COO)_6$ , where M is a trivalent metal (Fe, Cr, Sc, Co, Al, V, In...), which have six carboxylate branches (6-connected SBU) arranged in a trigonal prismatic form, linked by tetratopic (4-connected) organic ligand ABTC (3,3',5,5'-azobenzene tetracarboxylic acid) (30). As a result, it presents a cubic lattice, P-43n space group and a lattice parameter of 21.967 Å having two types of cavities or pores, as shown in Figure 2.3 (31).

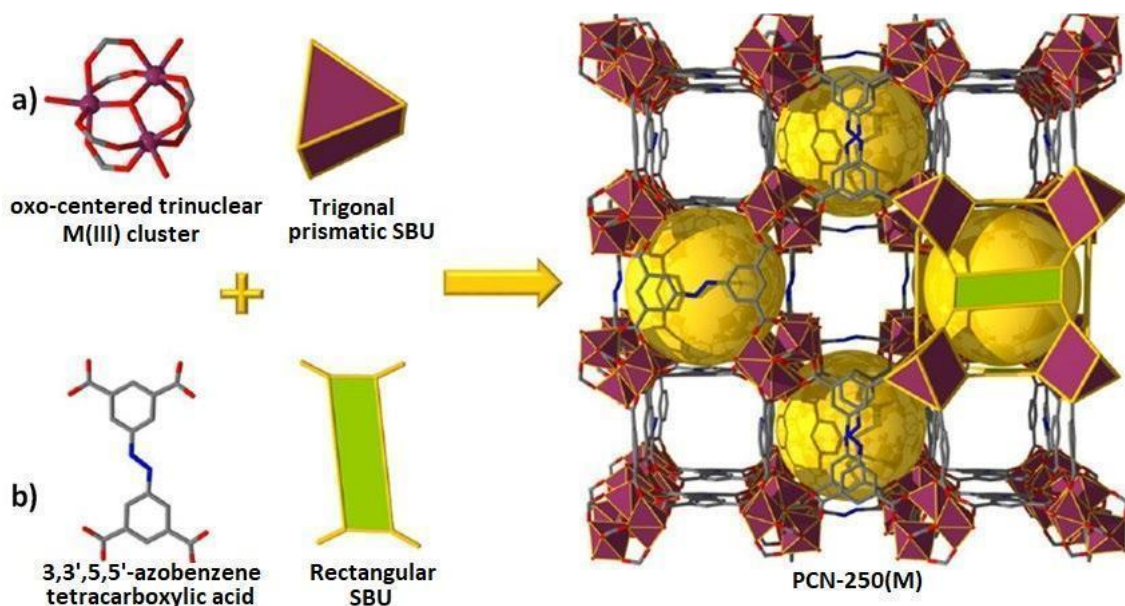


**Figure 2.3.** Structure of PCN-250 MOFs, taken from (32).

In relation to what was explained above, it can be observed that this MOF has a polynuclear cluster that exhibits chelation thanks to its carboxylate groups. On the other hand, the ligand also helps this chelation thanks to the carboxylate groups with which it binds to the cluster. These two factors are expected to help achieve high thermal and chemical stability in the structures.

The name PCN-250 usually refers specifically to the case in which cluster atoms are iron, that is,  $M = \text{Fe}$ . This MOF is also called **soc**-MOF, where the **soc** or “square-octahedron” denotation refers to crosslinking of square and octahedral structural units (6). For simplicity, PCN-250(M) notation will be used to distinguish the different isostructural MOFs.

The three studied isostructural MOFs have been: PCN-250(Fe) and PCN-250(Fe<sub>2</sub>Co). In addition to them, the functionalization of PCN-250(Fe) carried out by the in situ addition of imidazole: PCN-250(Fe-IM) has also been studied.

### 2.3. MOF synthesis

The most common procedure to synthesize MOFs is the solvothermal method, that consists in mixing the organic linker and the metal salt in a solvent. The resulting solution is placed inside a closed vessel, followed by heating at high temperature (usually over the boiling point of the solvent), with the consequent pressure increase (16, 33). When the synthesis method is called solvothermal, the solvent has to be an organic substance, such as dimethylformamide (DMF), dimethylsulfoxide (DMSO), dimethylacetamide (DMA), ethanol, among others. On the other hand, if water is used as the synthesis solvent, the procedure is called hydrothermal. It is important to highlight the possibility to use a mix of solvents that are miscible in each other, since solvent can be decisive to the formation and properties of the MOF. It is especially meaningful for the synthesis of water-sensitive MOFs in aqueous medium (34).

Reaction conditions also need to be taken into consideration, since they determine crystallinity, morphology, and reaction yield. The nature and concentration of reagents, nature of the solvent, medium pH, temperature, pressure, and time of reaction are just several examples (10, 35). Moreover, sometimes it is necessary to add modulators (HF, HNO<sub>3</sub>, HCl, benzoic acid, HAc, etc.) in order to achieve high crystalline structures and to control particle size. These acidic modulators form a previous SBU with the metal cluster that is later modified by the organic linker. The organic linker slowly substitutes the modulator molecules, controlling this way the MOF nucleation towards more crystalline structures (36).

Another key matter regarding MOF synthesis is the reaction scale-up. For the characterization techniques, a relatively large amount of MOF (around 500 mg) is needed. Achieving a large-scale reaction is not always a straightforward process since, for example, doubling the amount of reagents and the volume of solvent could lead to a decrease of yield or loss of crystallinity.

#### **2.4. MOFs for the removal of Emerging Organic Contaminants in water**

Water is essential for life as we know it, and it is one of the defining characteristics of our planet. As most of this water is in oceans, only a small portion of it is available to be extracted and employed. Over the last few decades, water contamination has become a serious issue due to new and hazardous anthropogenic contaminants. Despite the high number of wastewater treatment plants (WWTPs) in developed countries, water contamination is increasing. As a high number of new materials are being developed and applied in different sectors (agriculture, industry, etc.), pollutants in wastewater are diversifying (37, 38).

The so-called “emerging organic contaminants” (EOCs) are of particular concern, since they include not only previously known pollutants, but also these new substances with novel negative impacts for the planet and human health (39, 40). Hundreds of EOCs are detected in water analysis and come from a wide variety of sources: from pharmaceutical products to pesticides or industrial derivatives. Moreover, WWTPs are not equipped to remove them, or when equipped, the increasing loads overpass the capacity of the plant, and so EOCs enter the water resources from a lot of diverse routes (41).

Global population is reaching 7.9 billion people and the climate change effects (drought among them) are affecting our planet. It has been found that most of the global population struggles with water scarcity (42). Because of this, efficient water reuse after wastewater remediation should be a useful water resource, as water quality is essential for life and health (38).

In recent years, new treatment processes have been considered to remove EOCs from water (ozonization (43), activated carbon treatment (44), sono-degradation (45), chlorination (46), biodegradation (47), and inorganic heterogeneous catalysis (48)).

Among these, MOFs are one of the most promising materials since they have high sorption capacities, active sites where contaminants can be chemisorbed and degraded in catalytic processes. Moreover, they can be targeted designed for selective adsorption, synthesized at large scale, and adapted to different devices. MOFs have been tested for the removal of dyes, pharmaceuticals, herbicides, and pesticides, among others (38).

However, prior to the potential use of MOFs in water treatment, the material performance under real working conditions is a key parameter, determining whether real-world applications are viable or not. The composition, pH and temperature of real wastewater are important factors, because they may have an important influence on the MOF removal capacity (49). As the objective is to reduce contamination, eco-friendly MOFs are clearly desirable. Selecting safe and stable MOFs is mandatory for their use in water remediation, since many of them are built from toxic compounds that could be released to the environment upon MOF degradation, exacerbating the contamination issue. For industrial applications, green, economic, and efficient MOF synthesis and reusability are preferable (29, 49, 50).

### **3. OBJECTIVES**

---

El presente trabajo tiene como objetivo sintetizar y caracterizar tres diferentes MOFs de la familia PCN-250, con el objetivo final utilizarlos en estrategias de extracción de contaminantes del agua.

---

The main objective of this work is to synthesize and characterize a family of metal-organic frameworks with soc-like structure in order to use them for water remediation experiments. In this sense, specific objectives include the synthesis and characterization of these MOFs, followed by their use in adsorption experiments for different contaminants in water.

The synthesis of each MOF was scaled up and characterized by X-ray diffraction, thermal analysis (including TGA, DTG and DSC), infrared spectroscopy, and gas uptake techniques. Finally, the water contaminants adsorption studies were performed using

eight different contaminants. The obtained information from these results is needed to prove whether these MOFs have potential for water remediation purposes or not.

#### 4. EXPERIMENTAL SECTION

A continuación, se explican todos los procedimientos experimentales llevados a cabo, incluyendo la síntesis de los MOFs estudiados, su caracterización y los estudios de su uso en la adsorción de contaminantes.

##### 4.1. Reagents

Table 4.1 summarizes all the reagents (including organic linkers, metal salts, additives, and solvents) used for synthesizing the MOFs, as well as their abbreviations for further use. The organic linker was prepared following the procedures reported in the literature (51).

Name	Formula	Abbreviation
Iron (III) chloride hexahydrate	$\text{FeCl}_3 \cdot 6\text{H}_2\text{O}$	-
3,3',5,5'-azobenzene tetracarboxylic acid	$\text{C}_{16}\text{H}_{10}\text{N}_2\text{O}_8$	H <sub>4</sub> ABTC
Sodium acetate trihydrate	$\text{NaCH}_3\text{COO} \cdot 3\text{H}_2\text{O}$	-
Iron (III) nitrate nonahydrate	$\text{Fe}(\text{NO}_3)_3 \cdot 9\text{H}_2\text{O}$	-
Cobalt (II) nitrate hexahydrate	$\text{Co}(\text{NO}_3)_2 \cdot 6\text{H}_2\text{O}$	-
Imidazole	$\text{C}_3\text{H}_4\text{N}_2$	IM
<i>N, N</i> -dimethylformamide	$\text{C}_3\text{H}_7\text{NO}$	DMF
Acetic acid	$\text{CH}_3\text{COOH}$	-

**Table 4.1.** Reagents used in the synthesis of the MOFs.

## 4.2. Synthesis

The different PCN-250 MOFs were synthesized by scaling up the procedures reported in the scientific literature (30, 31, 52). In this section, all the synthetic procedures are explained in detail.

A solvothermal process is a synthetic method, similar to the hydrothermal procedure, where the reagents, dissolved in an organic solvent, are introduced in a closed reactor and heated under autogenous pressure. This method produces metastable phases that cannot be synthesized at room temperature or simply heating the reagents solution. The solvothermal reaction is carried out in a teflon-lined stainless steel vessel of 23 or 45 mL of capacity, depending on the volume of the solution.

First of all, it was necessary to weigh the reagents by using an analytical balance (with 1 mg of resolution). The metal salt was weighed, and then transferred to a glass beaker. After that, the solvent and the acidic modulator (both measured with a graduated cylinder), needed for the reaction, were added to the beaker. Then, the solution was put into an ultrasound bath to ensure the metal salt was completely dissolved. After that, the organic linker was weighed and mixed with the solution and placed again into the ultrasound bath to completely dissolve it. Finally, the mixture was transferred to an appropriate vessel. The synthetic temperature and the boiling point of the solvent must be considered, since a glass vial could not resist the pressure inside and break. If the procedure requires a temperature higher than the boiling point of the solvent, a solvothermal reactor must be used. The solvothermal reactor consists in a teflon vessel containing the reaction mixture and a stainless steel autoclave containing that teflon vessel. This reactor is adequate for carrying reactions that require high temperature and pressure conditions.

As the final step, the vessel was placed inside a preheated oven for the required time to maintain a uniform heat flow during the reaction time. When the time was finished, it was let to cool down. Then, the resulting mixture was gravity-filtered using the extra solvent to recollect all the solid product. Once the product was dried in air, it was carefully weighed and transferred to an Eppendorf tube.

The synthetic procedures were scaled up from reported procedures (30, 31, 52). In a first step, the reactions were scaled up by taking a previous efficient reaction and doubling the reagents quantities. A reaction is efficient if its yield, calculated as the

percentage of obtained product with respect to the theoretical maximum, is reasonably high and the products show a good crystallinity. Conditions modification may include doubling solvent volume, changing acidic modulator quantity, or even the solvent composition. The final scaled up synthesis procedures are presented below.

#### 4.2.1. PCN-250(Fe)

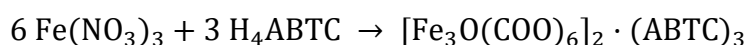
The reaction is:



where coordination water and byproducts have been omitted for clarity.

The PCN-250(Fe) MOF was synthesized by dissolving 240 mg of  $\text{FeCl}_3 \cdot 6\text{H}_2\text{O}$  (0.88 mmol) and 160 mg of  $\text{H}_4\text{ABTC}$  (0.44 mmol) in DMF (8 mL) and acetic acid (4 mL) in an ultrasound bath. The resulting mixture was transferred to a 23 mL solvothermal reactor and heated in an oven at 150 °C for 12 hours. After cooling down the reaction, microcrystals were obtained by filtration. They were washed with DMF and air dried. The color could vary from brown or orange to red (31).

An alternative synthesis was also tried, in which  $\text{Fe}(\text{NO}_3)_3 \cdot 9\text{H}_2\text{O}$  was the metal salt and water the solvent. The reaction is:



where coordination water and byproducts have been omitted for clarity.

This synthesis was performed by dissolving 90 mg of  $\text{Fe}(\text{NO}_3)_3 \cdot 9\text{H}_2\text{O}$  (0.50 mmol) and 90 mg of  $\text{H}_4\text{ABTC}$  (0.25 mmol) in water (10 mL) and acetic acid (1 mL) in an ultrasound bath. The resulting mixture was transferred to a 12 mL vial and heated in an oven at 80 °C for 24 hours. Finally, microcrystals were obtained by filtration (52). They were washed with DMF and air dried. Their appearance was similar to those synthesized in DMF.

#### 4.2.2. PCN-250( $\text{Fe}_2\text{Co}$ )

Previous to synthesizing the PCN-250( $\text{Fe}_2\text{Co}$ ) MOF, it was necessary to pre-form the  $\text{Fe}_2\text{Co}$  cluster. The reaction is:



where coordination water and byproducts have been omitted for clarity.

Thus, a solution containing 42 g of NaCH<sub>3</sub>COO (0.31 mol) in 70 mL of water was added to a filtered, stirred solution containing 8 g of Fe(NO<sub>3</sub>)<sub>3</sub>·9H<sub>2</sub>O (0.020 mol) and Co(NO<sub>3</sub>)<sub>2</sub>·6H<sub>2</sub>O (0.10 mol) in water (70 mL), and the brown precipitate was filtered off, washed with water and ethanol, and finally dried in air (30).

Once the pre-formed cluster was obtained, the MOF synthesis reaction is:

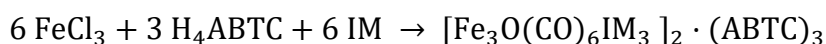


where coordination water and byproducts have been omitted for clarity.

The PCN-250(Fe<sub>2</sub>Co) MOF was synthesized by dissolving 213.2 mg of the Fe<sub>2</sub>Co preformed cluster (0.40 mmol) and 143.2 mg of H<sub>4</sub>ABTC (0.40 mmol) in DMF (8 mL) and acetic acid (4 mL) in an ultrasound bath. The resulting mixture was transferred to a 23 mL solvothermal reactor and heated in an oven at 130 °C for 24 hours. Finally, dark brown microcrystals were obtained by filtration. They were washed with DMF and air dried (30).

#### 4.2.3. PCN-250(Fe-IM)

The reaction is:



where coordination water and byproducts have been omitted for clarity.

The PCN-250(Fe-IM) MOF was synthesized by dissolving 240 mg of FeCl<sub>3</sub>·6H<sub>2</sub>O (0.88 mmol), 160 mg of H<sub>4</sub>ABTC (0.44 mmol) and 53.3 mg of imidazole (0.78 mmol) in DMF (8 mL) and acetic acid (4 mL) in an ultrasound bath. The resulting mixture was transferred to a 23 mL solvothermal reactor and heated in an oven at 150 °C for 12 hours. Finally, microcrystals were obtained by filtration (31). They were washed with DMF and air dried. Their appearance was equal to the PCN-250(Fe) ones.



MOF	Linker(s) (mg)	Metal (mg)	Solvent (mL)	Additive (mL)	T (°C)	t (h)	Yield* (%)
PCN-250(Fe)	H <sub>4</sub> ABTC (160)	FeCl <sub>3</sub> ·6H <sub>2</sub> O (240)	DMF (8)	HAc (4)	150	12	67
PCN-250(Fe)	H <sub>4</sub> ABTC (90)	Fe(NO <sub>3</sub> ) <sub>3</sub> ·9H <sub>2</sub> O (200)	Water (10)	HAc (1)	80	24	63
PCN-250(Fe <sub>2</sub> Co)	H <sub>4</sub> ABTC (143)	Fe <sub>2</sub> Co cluster (213)	DMF (8)	HAc (4)	130	24	64
PCN-250(Fe-IM)	H <sub>4</sub> ABTC (160) IM (53)	FeCl <sub>3</sub> ·6H <sub>2</sub> O (240)	DMF (8)	HAc (4)	150	12	67

\* Calculated as referred to the limiting reagent in each case

**Table 4.2.** Synthesis conditions of the MOFs and the yields obtained.

#### 4.2.4. Washing, solvent exchange, and thermal activation

After the synthesis, the MOFs were washed with the synthetic solvent to eliminate starting reagents in excess that could remain or soluble byproducts. After the washing, the solvent exchange procedure was performed by placing the MOF in a 100 mL beaker with acetone. Then, the beaker was closed with parafilm for three days. Then, the MOF was filtered off and placed in an oven equipped with a vacuum pump at 80 °C and 400 mbar for 24 hours. The vacuum pump helps to remove acetone molecules from the MOF pores.

### 4.3. Characterization

#### 4.3.1. Powder X-ray diffraction

The materials were characterized by powder X-ray diffraction (PXRD). In crystal solids, X-ray diffraction is governed by Bragg's law:

$$n \lambda = 2 d_{hkl} \sin(\theta)$$

where  $n$  is the diffraction order (1, 2, 3...),  $\lambda$  is the wavelength of incident radiation,  $d_{hkl}$  is the distance between two crystallographic planes with Miller indices (hkl), and  $\theta$  is the incidence angle.

Knowing the incident wavelength (usually copper,  $\lambda = 1,5405 \text{ \AA}$ ) and the diffraction angles, it is possible to determine the interplanar distance  $d_{hkl}$  and assign Miller indexes to all the reflections. Thus, information about lattice symmetry and parameters can be obtained. Since the X-ray diffraction pattern is unique for each compound, it can be used to identify the material. This can be done by comparison with simulated patterns.

PXRD of all MOFs were obtained using an Empyrean Diffractometer supplied by PANalytical (Eindhoven, The Netherlands). Data collection was carried out using Cu K $\alpha$  radiation ( $\lambda = 1.5418 \text{ \AA}$ ) over the angular range from  $5.01^\circ$  to  $80.00^\circ$  ( $0.025^\circ$  steps) with a total exposure time of 10 min.

#### **4.3.2. Water stability test**

The water stability of PCN-250( $\text{Fe}_2\text{Co}$ ) MOF was tested by placing 50 mg of activated sample in 50 mL of distilled water (pH = 7) inside a beaker for two different periods of time: one day and one week. After that, crystal structure integrity was checked using PXRD while compared with previous diffraction patterns.

#### **4.3.3. Thermal analysis**

Thermal analysis can provide important information about physical and chemical phenomena, such as phase transitions, decomposition, oxidation, reduction, and evaporation. In this sense, thermogravimetric analysis (TGA) and differential scanning calorimetry (DSC) were performed.

TGA consists in measuring the mass variation of a sample while the temperature changes. A typical thermogravimetric analyzer consists in a precision balance with a sample vessel located inside a tubular furnace with a programmable temperature controller. These tubular furnaces can usually reach up to  $1500^\circ\text{C}$  or even  $2000^\circ\text{C}$ . As the mass changes, so does the sample pan position. That movement is measured with a photosensor, and it is translated to mass variation by a previous calibration. The

atmosphere in which the process takes place is important since, for example, oxygen makes oxidation possible. When performing the analysis under an inert atmosphere, nitrogen could be a good choice. This analysis gives two graphics: a plot of the mass as a function of the temperature (TGA) and its derivative.

DSC consists in measuring the amount of energy absorbed or emitted by the mass as a function of the temperature. Both materials are introduced in the same oven with temperature sensors, so that electrical power is supplied to the sample to keep its temperature to be the same as the reference material. The plot represents the power supplied as a function of the temperature; thus, a DSC curve is obtained.

Thermal analysis of all MOFs was carried out by TGA and DSC. In this case, a Discovery SDT 650 thermal analyzer supplied by TA Instruments was used. The measure was carried out by using a platinum (Pt) vessel under N<sub>2</sub> atmosphere. The temperature was increased at a rate of 10 °C·min<sup>-1</sup> from 25 °C to 800 °C for 128 min.

The main objective is to study the thermal stability of the MOFs, determine the temperature at which they start to decompose, and the efficacy of the activation process.

#### **4.3.4. Infrared spectroscopy**

Infrared (IR) spectroscopy constitutes the study of the interaction between infrared radiation and matter. IR radiation is not energetic enough to excite electron states in the sample, instead rotational and vibrational states are excited by using this radiation. In the case of non-linear molecules with N number of atoms, the number of vibrational modes in which it can vibrate is  $3N - 6$ , each one associated with a certain movement (stretching or bending) and energy, which corresponds to the energy of the IR radiation that can excite it. For these states to be IR active, they must be associated with changes in the dipole moment.

An IR spectrum consists in plotting the transmittance as a function of the wavenumber. With this data, it is possible to identify which frequencies excite the vibrational states and, therefore, the associated energies. Thus, it is possible to identify which chemical substances or functional groups are present in the sample. This can be done because functional groups give raise to characteristic absorption bands, both in frequency and intensity.

Fourier transform infrared (FTIR) spectrometers are commonly used. These spectrometers irradiate the sample with all the IR frequencies at the same time, and then measure the non-absorbed radiation. The Fourier transform is a mathematical operation that transforms a time-dependent function into the corresponding frequency-dependent function. This way, the FTIR spectrometers use it to decompose the non-absorbed radiation into the frequencies that compose it. By comparison with the irradiation data, these spectrometers can tell how much of each frequency was absorbed. By comparison, non-FTIR spectrometers are much slower since they do not irradiate with all the frequencies at once but do a monochromatic frequency sweep.

A Bruker attenuated total reflectance (ATR) Fourier transform-infrared (FTIR) spectroscope was used in the identification of the functional groups present in the MOFs. The goal is to check the presence of DMF, H<sub>4</sub>ABTC, and cluster contributions to the spectrum. DMF exchange with acetone as a part of the activation process is also going to be checked.

#### **4.3.5. Gas adsorption**

The porosity of a material is defined as the ratio of the volume of the pores to the total volume occupied by the solid (%) or its mass ( $\text{cm}^3 \cdot \text{g}^{-1}$ ). Since MOF pores can be accessed by guest molecules, they are commonly described by their gas uptake properties. N<sub>2</sub> is the most employed gas, since it does not chemically react with most samples. These gas uptake properties are derived from adsorption-desorption isotherms and are usually interpreted through Brunauer-Emmett-Teller (BET) theory.

Most of the isotherms can be classified following the IUPAC recommendations into six groups: I(a), I(b), II, III, IV(a), IV(b), V and VI (53). When adsorbate-adsorbate interactions are small with respect to adsorbate-adsorbent interactions, type I, II, IV and VI isotherms are obtained. Otherwise, type III and V isotherms are obtained. This classification is tentative, since there are isotherms that do not belong to just one type.

The BET theory is widely used to describe the physical adsorption of gas molecules by a porous solid surface, and it can be used to determine the specific surface area of a material. In particular, BET theory applies to systems where multilayer adsorption takes place, whereas other models like the Langmuir model only contemplate

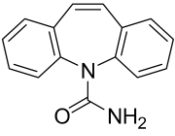
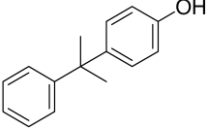
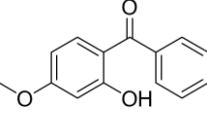
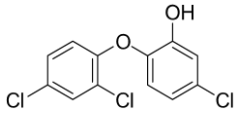
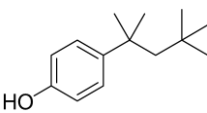
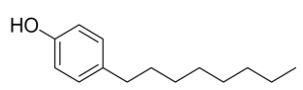
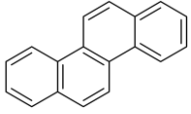
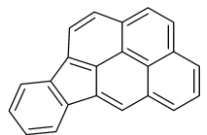
monolayer adsorption. Specific surface area is a scale-dependent property, so this quantity may vary from one sample to another of the same material if the average grain size is different. This surface area is related to the adsorption behavior of the material, because it depends on the size, accessibility, and distribution of its pores.

The nitrogen adsorption isotherms were measured using a Gemini V2365 Model, supplied by Micrometrics (Norcross, GA, USA), surface area analyzer at 77 K in the range  $0.01 \leq P/P_0 \leq 1.00$ .

#### **4.4. Analytical performance**

All the synthesized MOFs were tested as sorbents in an analytical microextraction procedure for a group of contaminants quite different structurally (see Table 4.3). Microextraction procedures are extraction techniques in which the volume of the extracting phase is very small compared to the sample volume. Moreover, in many cases only a small amount of the analyte is extracted (54). In the case that the adsorbent is a solid, the procedure is called solid-phase extraction, SPE. Common SPE techniques involve passing the liquid sample through a column containing a sorbent porous material that interacts with the analytes and separates them from the sample. One of the variations of the technique is to put the sorbent in direct contact with the sample, dispersing it into the liquid instead of packing it in a column. This variation is called dispersive SPE, or dSPE. Moreover, when this technique involves small quantities of sorbent (mg or  $\mu\text{g}$ ) is called dispersive micro-solid-phase extraction ( $\mu$ -dSPE) (55).

In this work, the  $\mu$ -dSPE method was performed under optimum conditions that were previously published in past studies by the research group (56), as shown in Figure 4.1. The optimum conditions ensure to have the best extraction performance of the MOF, because they involve relatively high MOF quantity, analyte concentration and sorbent-analytes interaction.

Analyte (abbreviation) Type	Structure	MF <sup>1</sup> MW <sup>2</sup> (g·mol <sup>-1</sup> )	pK <sub>a</sub>	Log K <sub>ow</sub> <sup>3</sup>
Carbamazepine (Cbz) PPCP <sup>4</sup>		C <sub>15</sub> H <sub>12</sub> N <sub>2</sub> O 236.27	13.9	1.90
4-Cumylphenol (4-CuP) EDC <sup>5</sup>		C <sub>15</sub> H <sub>16</sub> O 212.29	10.6	4.24
Benzophenone-3 (BP-3) PPCP		C <sub>14</sub> H <sub>12</sub> O <sub>3</sub> 228.24	7.6	4.00
Triclosan (Tr) PPCP		C <sub>12</sub> H <sub>7</sub> Cl <sub>3</sub> O <sub>2</sub> 289.54	7.8	5.34
4- <i>tert</i> -Octylphenol (4-t-OP) EDC		C <sub>14</sub> H <sub>22</sub> O 206.32	10.2	5.18
4-Octylphenol (4-OP) EDC		C <sub>14</sub> H <sub>22</sub> O 206.32	10.2	5.63
Chrysene (Chy) PAH <sup>6</sup>		C <sub>18</sub> H <sub>12</sub> 228.29	-	5.73
Indeno[1,2,3-cd] pyrene (Ind) PAH		C <sub>22</sub> H <sub>12</sub> 276.33	-	6.65

### Abbreviations

**MF:** molecular formula, **MW:** molecular weight, **K<sub>ow</sub>:** Octanol/water partition coefficient, **PPCP:** Pharmaceutical and personal care product, **EDC:** endocrine disrupting chemical, **PAH:** Polycyclic aromatic hydrocarbon.

**Table 4.3.** Structures and several physicochemical properties of the analytes studied (SciFinder® 2019).

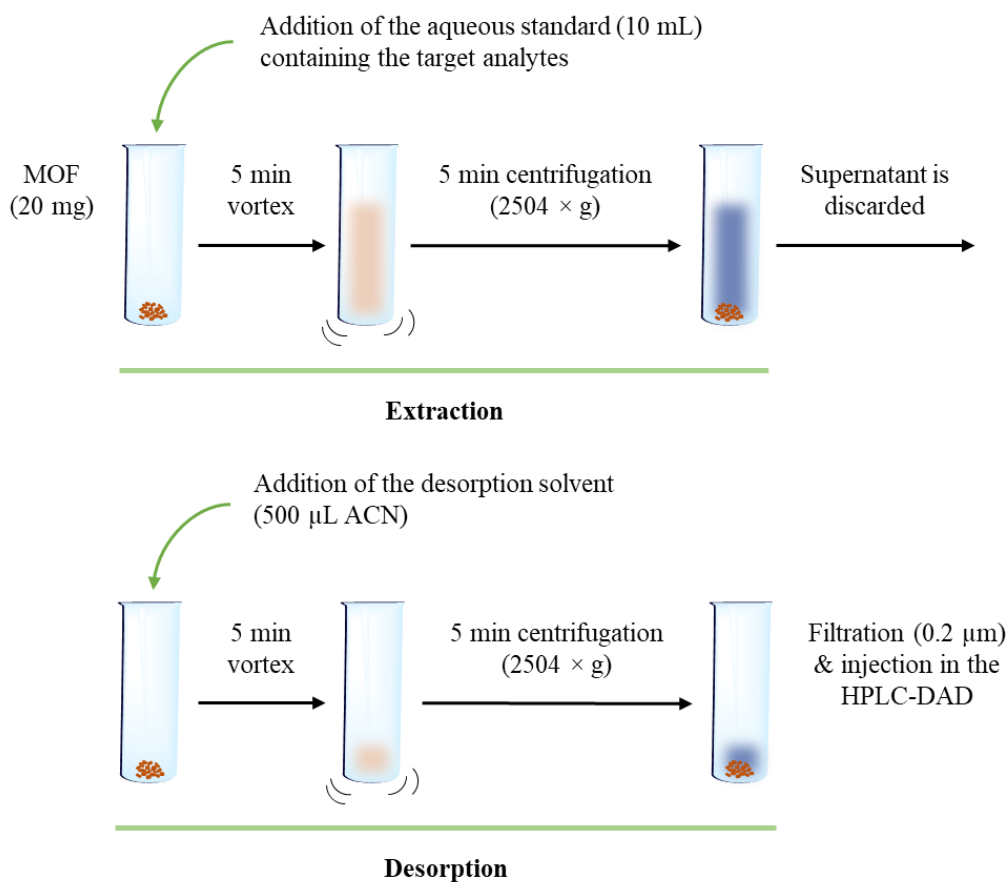


**Figure 4.1.**  $\mu$ -dSPE method performed under optimum conditions.

This microextraction method was combined with high performance liquid chromatography (HPLC) and diode array detection (DAD) to obtain the chromatographic data. HPLC consists in pumping the sample in a solvent through a column with chromatographic packing material, known as the stationary phase. The sample constituent's retention time varies depending on the interaction with the stationary phase, so the different substances will exit the column at different times. The exit flow is measured using a deuterium lamp and a multiwavelength UV-vis diode array detector. The exit time and UV spectra data can be used to identify the composition of the exit flow and the concentration of those substances. Knowing the starting and the final concentrations of each contaminant, the extraction rates can be calculated (57).

## 5. RESULTS AND DISCUSSION

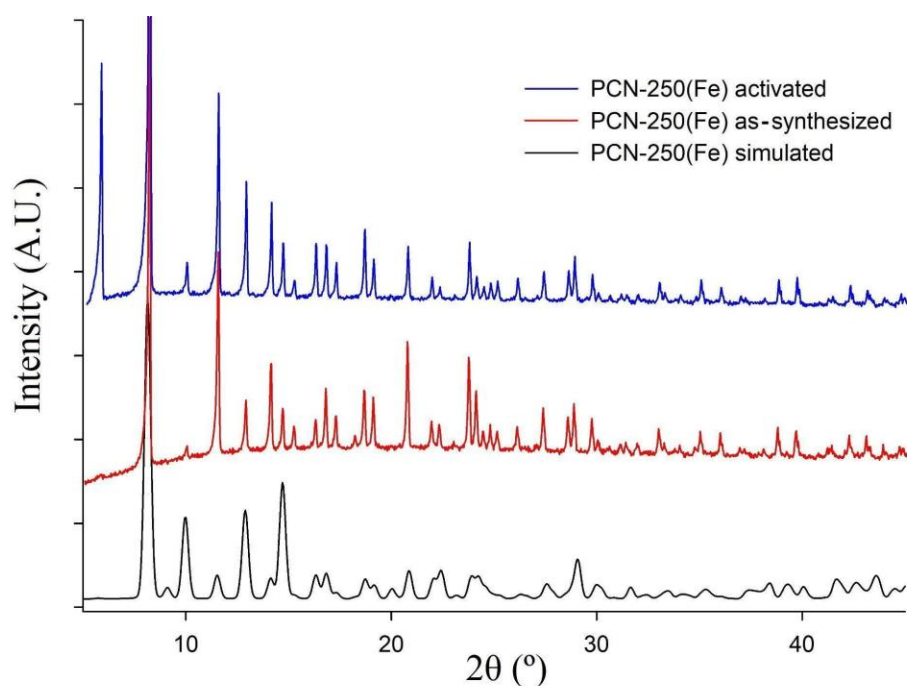
---

En este apartado se recopilan e interpretan los resultados obtenidos, relativos a la caracterización de los MOFs y su desempeño en las pruebas analíticas de extracción.

---

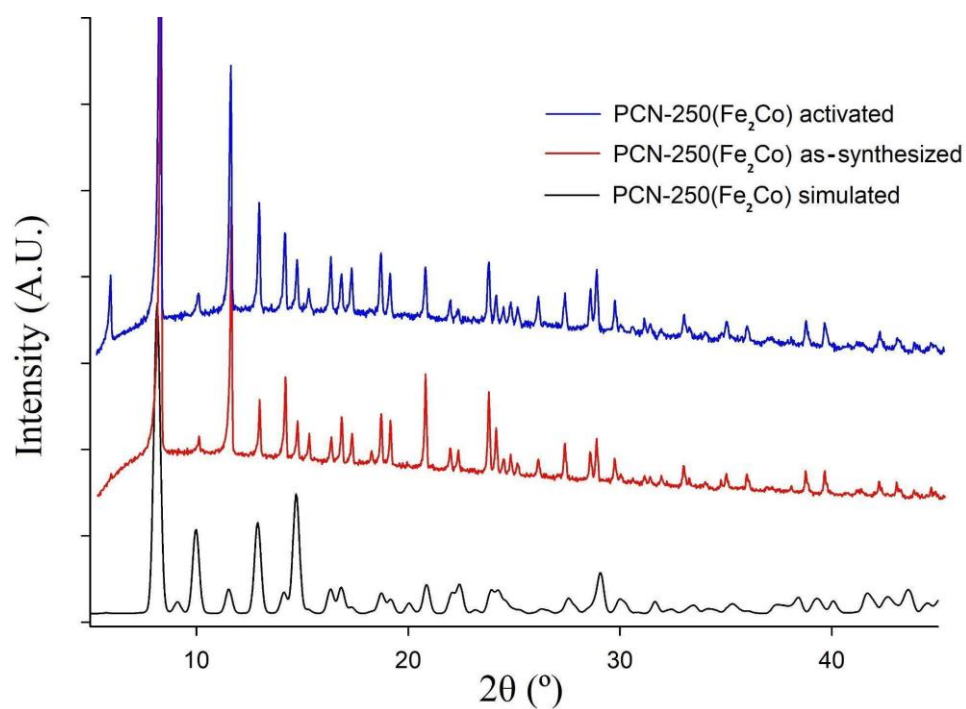
### 5.1. PXRD patterns

Figures 5.1, 5.2 and 5.3 show the diffraction patterns of as-synthesized and activated MOFs. A simulated pattern is included in each graphic with comparative purposes. The simulated patterns were represented with the FullProf Suite Crystallographic Calculator *software*, by using the crystallographic data found in the Cambridge Crystallographic Database Center (CCDC) (58).

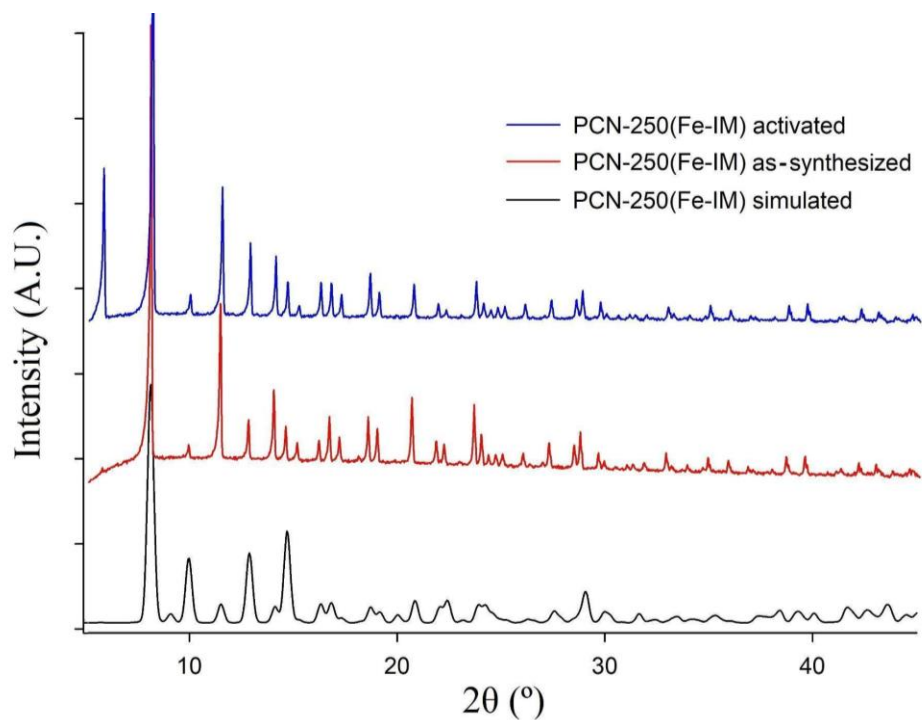


**Figure 5.1.** PXRD patterns of both the as-synthesized and the activated samples corresponding to the PCN-250(Fe) MOF, and its simulated pattern.





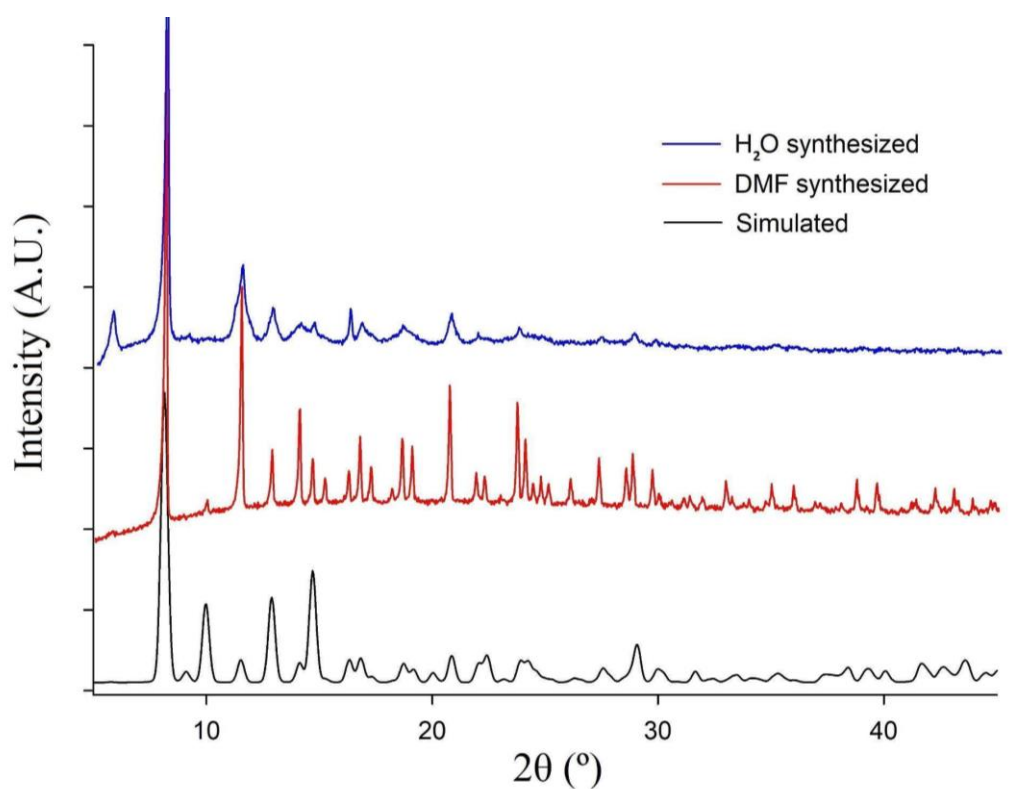
**Figure 5.2.** PXRD patterns of both the as-synthesized and the activated samples corresponding to the PCN-250( $\text{Fe}_2\text{Co}$ ) MOF, and its simulated pattern.



**Figure 5.3.** PXRD patterns of both the as-synthesized and the activated samples corresponding to the PCN-250( $\text{Fe-IM}$ ) MOF, and its simulated pattern.

All diffraction patterns corresponding to as-synthesized MOFs coincide with the simulated ones, so it can be concluded that all the MOFs were successfully synthesized. A proper signal-noise relation was also achieved, and the peaks are intense and relatively thin, showing that the MOFs are highly crystalline. This is because, according to Bragg's Law, if the diffraction angle is not well defined (broad peak) the interplanar distance is neither, as the rest of parameters are fixed, implying less crystallinity.

A comparison between the as-synthesized and the activated samples shows that the activation process did not modify the crystalline structure, since all the peaks remain with the same position and intensities as those from the as-synthesized sample. However, one extra peak appears at low  $2\theta$  angles after the activation process is performed. It is also present in the non-activated sample, but its intensity is small because the disordered solvent molecules contribution to the structure factor ( $F$ ) does not lead to a high intensity. After the removal, this contribution is not there anymore, so it allows this peak to have a higher intensity.



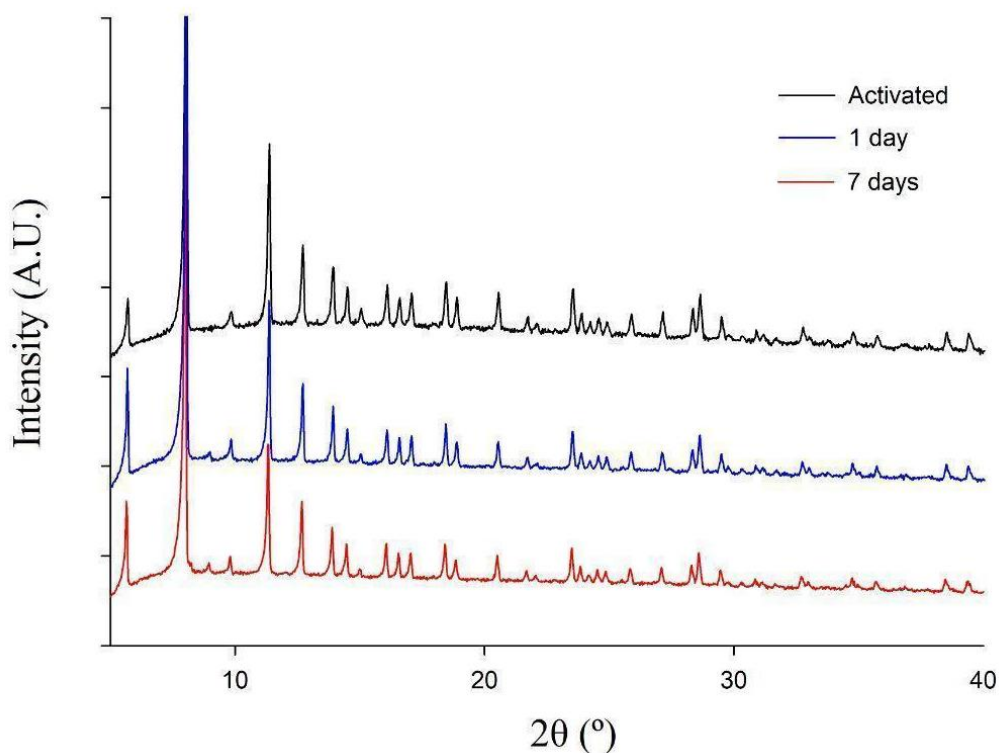
**Figure 5.4.** PXRD patterns of both the water synthesized and the DMF synthesized samples corresponding to the PCN-250(Fe) MOF, and its simulated pattern.

Figure 5.4 shows the diffractogram of the PCN-250(Fe) MOF synthesized in water. As comparison, a diffraction pattern of the same MOF synthesized in DMF and

the simulated one are also included. The peaks of the MOF synthesized in water are remarkably broader and less intense than the peaks of that same MOF synthesized in DMF, even some peaks cannot be differentiated from the background noise. The same peak at low angles that was found in the diffractogram corresponding to the activated MOF that was synthesized in DMF (see Figure 5.1) is also present in Figure 5.4, but much less intense. The explanation is similar to the previous one, and it can be found in the simulated pattern.

## 5.2. Water stability test

Figure 5.5 shows the water stability test diffractograms of the PCN-250( $\text{Fe}_2\text{Co}$ ) MOF. There is no perceptible loss of crystallinity or structure collapse after up to seven days of water exposure. An extra peak also appears right after the main peak.



**Figure 5.5.** Diffractograms of the PCN-250( $\text{Fe}_2\text{Co}$ ) MOF samples: activated and exposed to distilled water for one day and one week.

### 5.3. IR spectroscopy

The IR spectrum of the PCN-250(Fe) MOF is shown in Figure 5.6. Main absorption peaks or bands are associated with the contribution of different constituents (see Table 5.1). Some of them are associated with more than one constituent, as some of these have similar functional groups or chemical bonds, such as C-C, C-H, C-N or C=O.

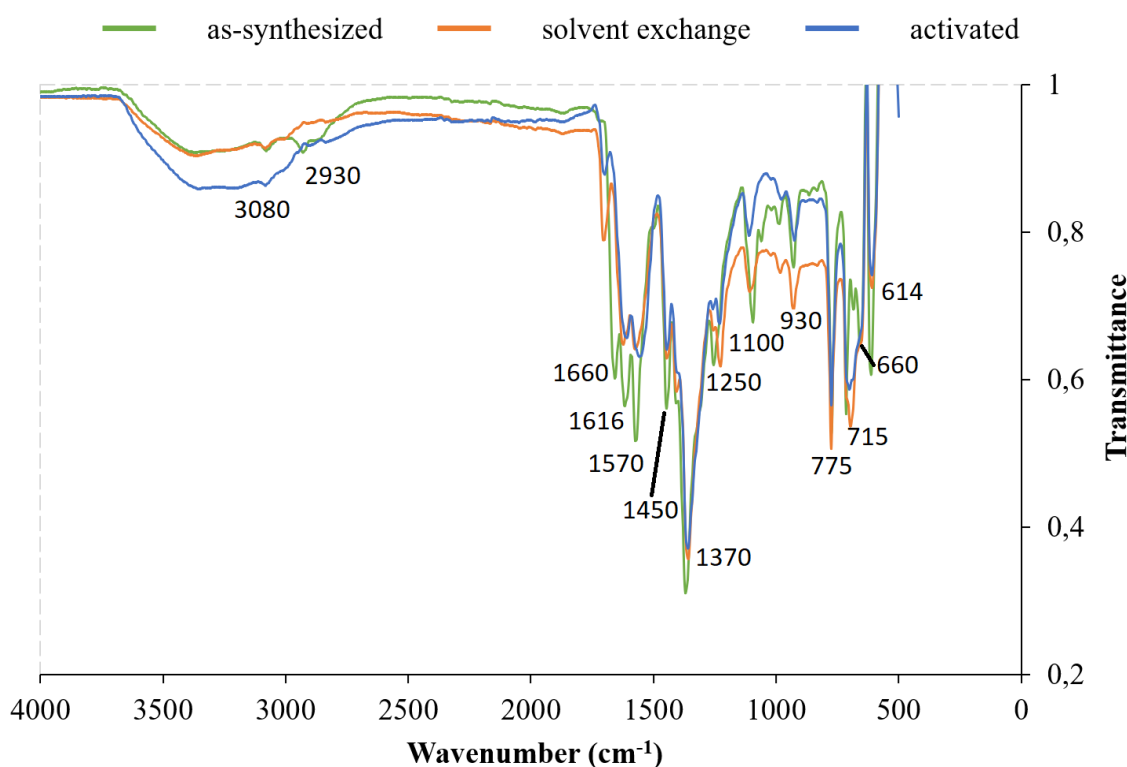


**Figure 5.6.** IR spectrum of the PCN-250(Fe) MOF as-synthesized, after solvent exchange with acetone and activated.

After the solvent exchange, the peaks at 1100 cm<sup>-1</sup> and 1660 cm<sup>-1</sup> lose intensity. These peaks are due to the C-N group, which is present both in the DMF and the H<sub>4</sub>ABTC, that is why they do not disappear, but lose intensity after the withdrawal of DMF molecules from the pores of the MOF. The difference between the acetone exchanged sample and the full activated sample is not obvious, since the acetone has all its bonds in common with other constituents, such as the C=O present in the ligand.

Peak (cm <sup>-1</sup> )	Functional group	Constituent
614 660	Fe-O (stretching)	cluster
715 775	benzene	ligand
930	Fe-O (bending)	cluster
1100 1250	C-N (stretching)	solvent, ligand
1370 1450 1570 1616	COOH	ligand
1660	C-N	solvent, ligand
2930 3080	O-H (stretching)	ligand

**Table 5.1.** IR spectrum peaks association with the corresponding functional groups and constituents.

#### 5.4. Thermal analysis

TGA curves of the MOFs are shown in Figures 5.7 to 5.9.

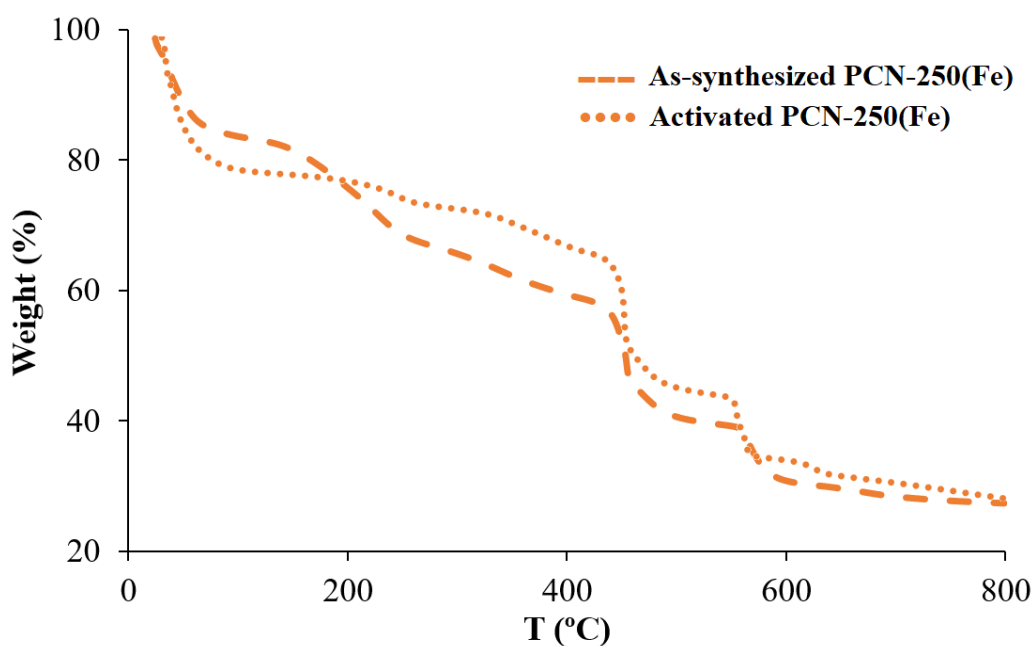


**Figure 5.7.** TGA of the as-synthesized and activated PCN-250(Fe) MOF.

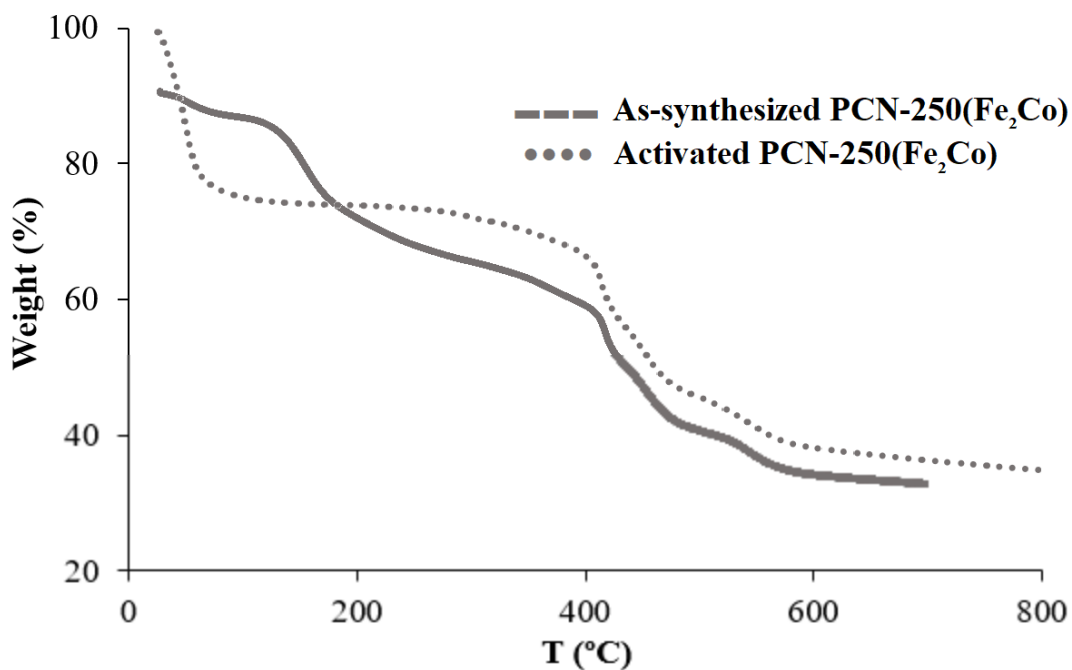


**Figure 5.8.** Thermal analysis of the as-synthesized PCN-250(Fe<sub>2</sub>Co) MOF.

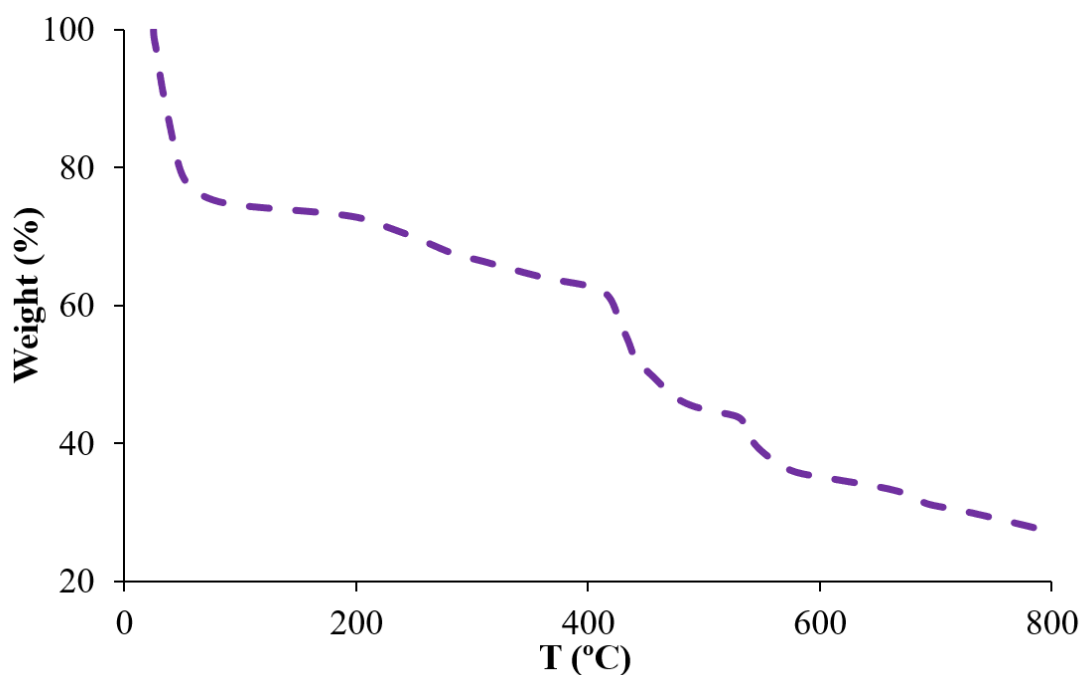


**Figure 5.9.** Thermal analysis of the as-synthesized PCN-250(Fe-IM) MOF.

The mass drops below 250 °C are usually due to the evaporation of solvent particles. Acetone boils at 56 °C whereas acetic acid (modulator) and DMF (solvent) boils at 118 and 153 °C, respectively. Their liberation may take place at higher temperatures,

since they are trapped inside the MOF pores, where the interaction raises the temperature necessary for their liberation. DMF evaporation may correspond to the 200 °C mass drop, since the band cannot be found in the activated samples. Around 250 °C, it seems to be another peak in all the samples that overlaps with the DMF evaporation in non-activated samples. According to the literature, this band corresponds to a new cluster oxidation state (59). Finally, the MOF decomposition takes place above 400 °C, where mass drops are around 425 °C and 675 °C. In general, all the MOFs are thermal stable in the range of 100 °C to 400 °C.

### 5.5. Gas uptake

The gas uptake isotherms are represented in Figures 5.12 and 5.13.

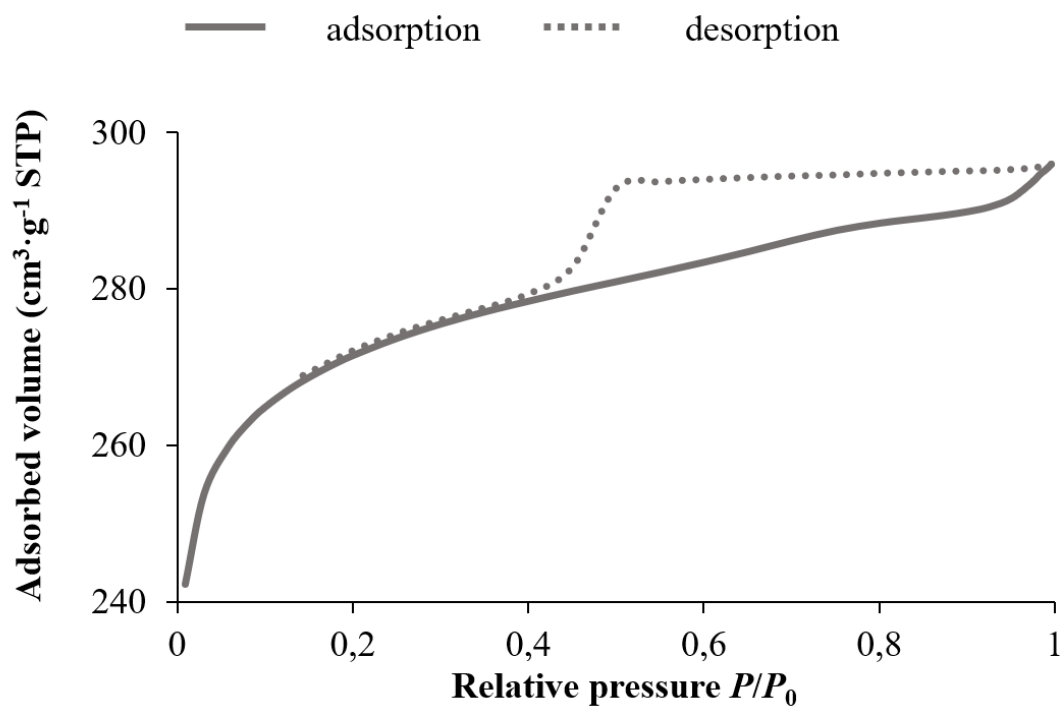


**Figure 5.12.** Adsorption and desorption isotherms of the PCN-250( $\text{Fe}_2\text{Co}$ ) MOF.

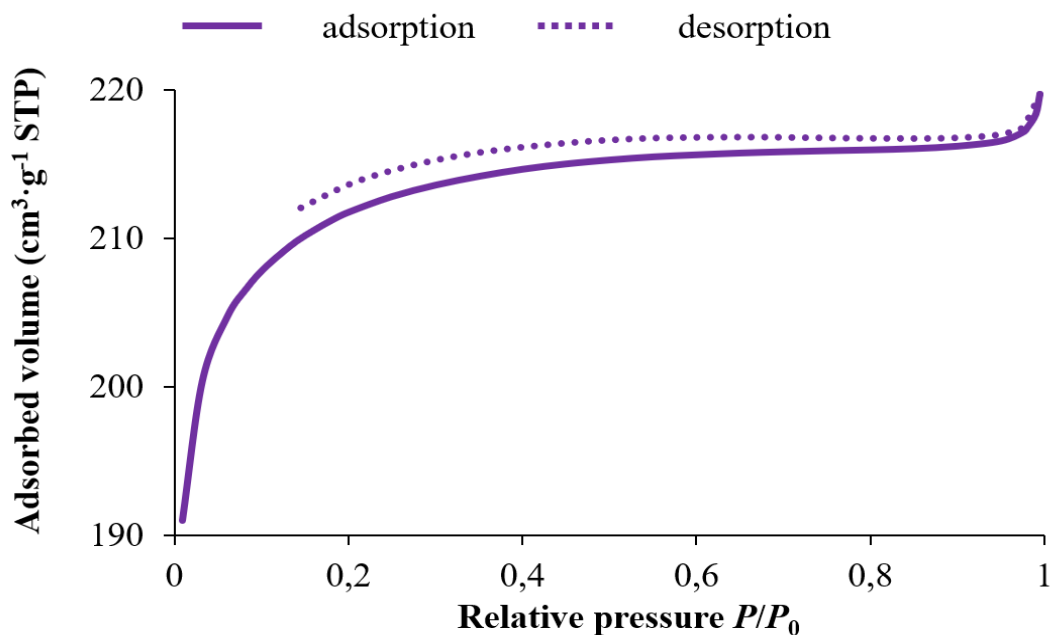


**Figure 5.13.** Adsorption and desorption isotherms of the PCN-250(Fe-IM) MOF.

The PCN-250( $\text{Fe}_2\text{Co}$ ) MOF isotherm belongs to the IV(a) IUPAC type. This plot is characteristic of mesoporous solids. In this kind of materials, adsorptive molecules close to two walls of a pore experience enhanced attractive forces, which lead to condensation at relatively low pressures. At the medium part of the curve, pores fill with multilayers of adsorptive molecules, and at the end of the curve pores fill with condensate molecules. The occurrence of a wide hysteresis loop indicates that evaporation from a pore is a distinctly different process from condensation within it. This difference causes the desorption curve to lag respect to the adsorption curve (60). The BET theory application yields a BET specific surface area of  $881 \text{ m}^2/\text{g}$ .

The PCN-250(Fe-IM) MOF isotherm belongs to the I(b) IUPAC type. This isotherm shape is characteristic of microporous solids. In this kind of materials, the curve rises almost vertically, levels out to a horizontal section and then rises again as it approaches saturation and bulk condensation begins to occur. Adsorption takes place by micropore filling under a low relative pressure driving force. Once the micropores have filled, no more adsorption takes place until condensation takes place (60). BET theory application yields a BET specific surface area of  $710 \text{ m}^2/\text{g}$ .



## 5.6. Analytical performance

As shown in Figure 5.15, it is clear that the PCN-250(Fe) has been the best performing MOF, followed by the PCN-250(Fe-IM). In general, extraction rates for these MOFs are relatively high, reaching more than 70% in half of the analytes. In general, the MOFs show a better performance towards polycyclic aromatic hydrocarbons and triclosan structures, showing the importance of the contaminants structure in the extraction performance. The reproducibility is also very good, as the triplicate studies led to low errors.

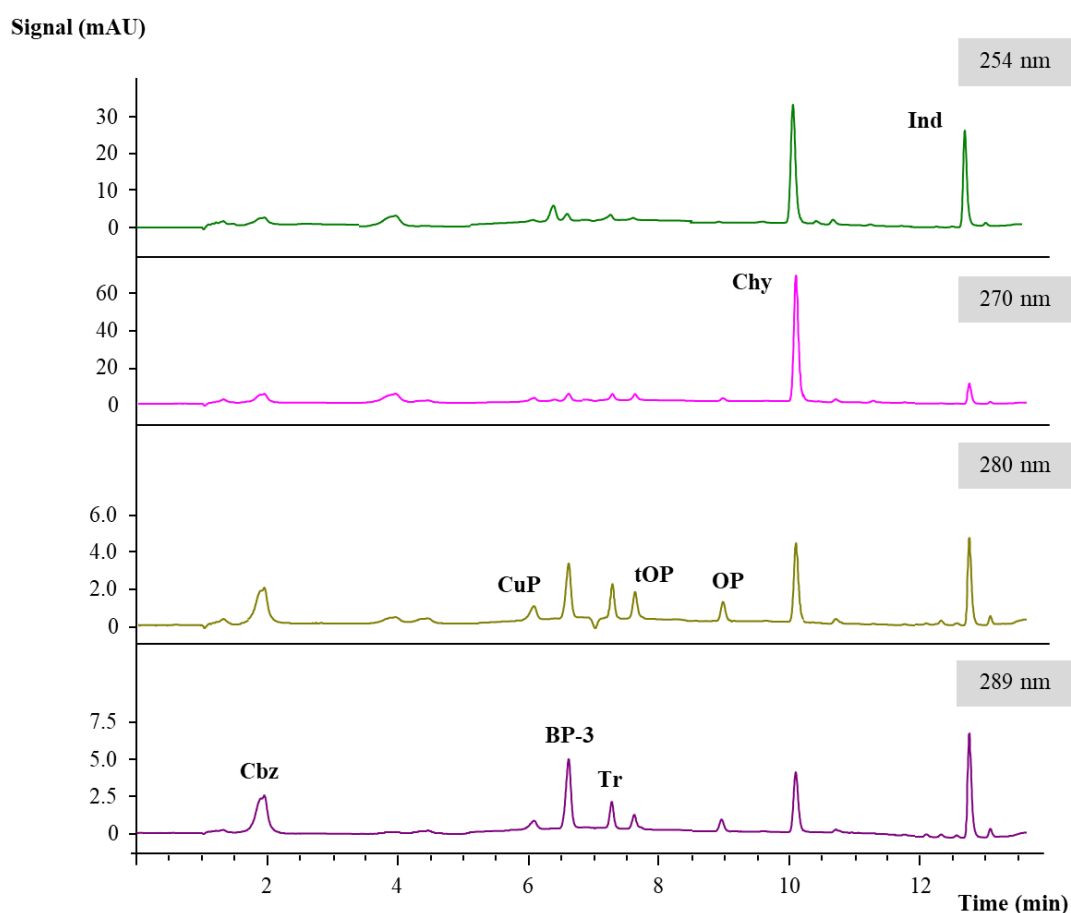


**Figure 5.14.** Chromatogram of the exit flow.

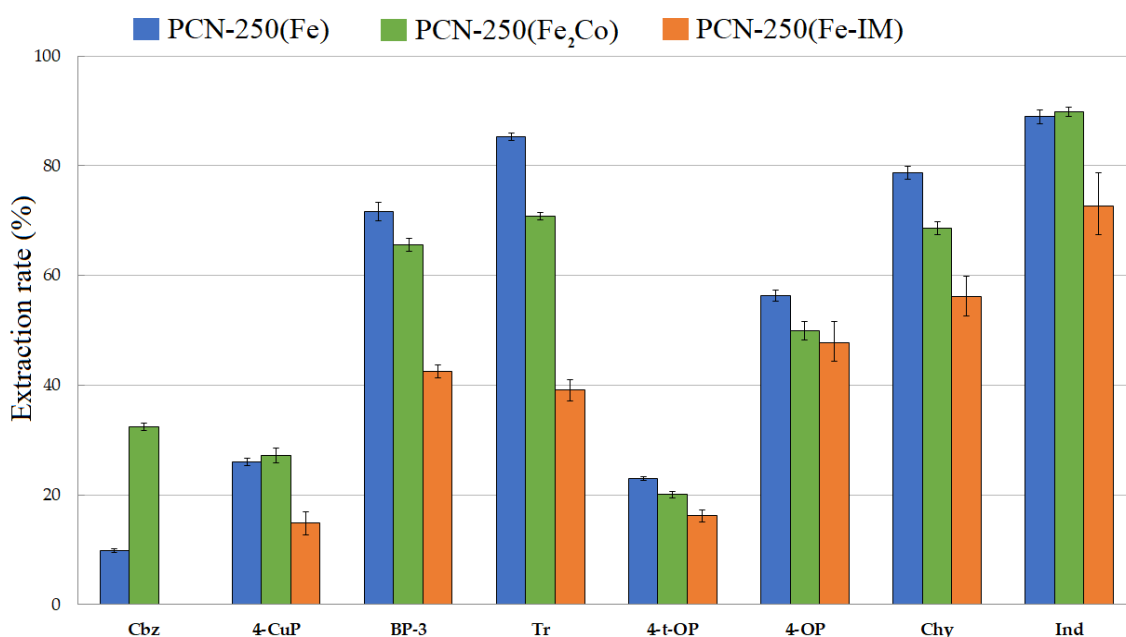


**Figure 5.15.** Water contaminants extraction rate of the MOFs for each contaminant.

In the case of the carbamazepine (Cbz), the PCN-250(Fe-IM) MOF has a much better performance than the PCN-250(Fe) MOF. This may be due to the hydrogen bonds that take place inside the pores thanks to the imidazole polar functionalization. These hydrogen bonds may also take place in other contaminants, as most of them have polar functional groups like OH or Cl, but the lower specific surface area of PCN-250(Fe-IM) and narrower pore size (31) may counter this effect. There is not a straightforward reason between the PCN-250(Fe) and PCN-250(Fe<sub>2</sub>Co) MOFs to account for the differences observed in extraction (Fig. 5.15). The cobalt ion does not seem to exert such profound changes in the electronic configuration of the cluster to increase or decrease the interactions with the analytes. Indeed, it has been observed in previous studies that the specific surface areas are different: 989 m<sup>2</sup>/g for the PCN-250(Fe) (31) and 881 m<sup>2</sup>/g for the PCN-250(Fe<sub>2</sub>Co), but this does not explain these differences. Further research regarding the analyte-MOF interactions should be conducted to clarify this point.

## 6. CONCLUSIONS

---

Se ha conseguido sintetizar, activar y caracterizar satisfactoriamente todos los MOFs, mostrando buenas propiedades de estabilidad y porosidad. Además, su desempeño en las pruebas analíticas para la eliminación de contaminantes hace del MOF PCN-250(Fe) un prometedor candidato en futuros estudios del grupo de investigación MAT4LL.

---

In accordance with the objectives of the present work, the three studied MOFs have been successfully synthesized, characterized, and tested for the removal of a group of water contaminants, in order to check their potential for water remediation. The reported data obtained from the different methods lead to the following conclusions.

First, the coincidence between the as-synthesized samples and the simulated patterns confirm that all MOFs have been successfully synthesized, with a reasonably good yield and crystallinity. The activation process did not compromise the crystalline structure, as shown in the comparison between the as-synthesized and activated samples diffraction patterns. The process successfully removed solvent molecules from the pores, as shown in the IR spectrum and the thermal analysis. Moreover, the thermal analysis and water stability tests lead to conclude that these structures are very stable to temperature from 100 °C to 400 °C and to distilled water exposure for at least 7 days. Gas uptake data indicates a high surface specific area, associated with high porosity of the samples. Finally, the relatively high adsorption rates for the different contaminants in water indicate that the PCN-250(Fe) MOF has a good potential for water remediation and will be used in future investigations by the MAT4LL research group.

## 7. REFERENCES

- (1) James, S. L. Metal-Organic Frameworks. *Chem. Soc. Rev.* **2003**, 32, 276-288.
- (2) Salcedo-Abraira, P.; Horcajada, P. Redes Metal-Orgánicas: Tipos, síntesis, modificaciones y materiales compuestos, *An. Quím.* **2021**, 117 (2), 92-99.
- (3) Moulton, B.; Zaworotko, M. J. From Molecules to Crystal Engineering: Supramolecular Isomerism and Polymorphism in Network Solids. *Chem. Rev.* **2001**, 101, 1629–1658.
- (4) Bell, D. S. The promise of Metal-Organic Frameworks for use in liquid chromatography, *LCGC North Am.* **2018**, 36(6), 352-354.
- (5) O’Keefe, M.; Peskov, M. A.; Ramsden, S. J.; Yaghi, O. M. The reticular Chemistry Structure Resource (RCSR) of, and Symbols for, Crystal Nets. *Acc. Chem. Res.* **2008**, 41, 12, 1782–1789.
- (6) Kim, D.; Liua, X.; Lah, M. S.; Topology analysis of metal–organic frameworks based on metal–organic polyhedra as secondary or tertiary building units. *Inorg. Chem. Front.* **2015**, 2, 336-360.
- (7) Hoskins, B. F.; Robson, R. Infinite Polymeric Frameworks Consisting of Three Dimensionally Linked Rod-like Segments. *J. Am. Chem. Soc.* **1989**, 111, 5962-5964.
- (8) Yaghi, O. M.; Kalmutzki, M. J.; Dierks, C. S. Introduction to Reticular Chemistry. *Wiley-VCH* **2019**.
- (9) Drout, R. J.; Robison, L.; Chen, Z.; Islamoglu, T.; Farha, O. K. Zirconium metal-organic frameworks for organic pollutant adsorption. *Tr. in Chem.* **2019**, 1 (3), 304-317.
- (10) McKinstry, C.; Cussen, E. J.; Fletcher, A. J.; Patwardhan, S. V.; Sefcik, J. Effect of Synthesis Conditions on Formation Pathways of Metal Organic Framework (MOF-5) Crystals. *Cryst. Growth Des.* **2013**, 13, 12, 5481–5486.
- (11) Kalaj, M.; Cohen, S. M. Postsynthetic Modification: An Enabling Technology for the Advancement of Metal–Organic Frameworks. *ACS Cent. Sci.* **2020**, 6, 7, 1046–1057.
- (12) Yin, Z.; Wan, S.; Yang, J.; Kurmoo, M.; Zeng, M.-H. Recent advances in post-synthetic modification of metal–organic frameworks: new types and tandem reactions. *Coord. Chem. Rev.* **2019**, 378, 500-512.
- (13) Tanabea, K. K.; Cohen, S. M. Postsynthetic modification of metal–organic frameworks—a progress report. *Chem. Soc. Rev.* **2011**, 40, 498-519.
- (14) Ding, M.; Cai, X.; Jiang, H.-L. Improving MOF stability: approaches and applications. *Chem. Sci.*, **2019**, 10, 10209-10230.

- (15) Healy, C.; Patil, K. M.; Wilson, B. H.; Hermanspahn, L.; Harvey-Reid, N. C.; Howard, B. I.; Kleinjan, C.; Kolien, J.; Payet, F.; Telfer, S. G.; Kruger, P. E.; Bennett, T. D. The thermal stability of metal-organic frameworks. *Coord. Chem. Rev.* **2020**, 419, 213388.
- (16) Howarth, A. J.; Peters, A. W.; Vermeulen, N. A.; Wang, T. C.; Hupp, J. T.; Farha, O. K. Best Practices for the Synthesis, Activation, and Characterization of Metal–Organic Frameworks. *Chem. of Mat.* **2017**, 29 (1), 26-39.
- (17) Li, N.; Xu, J.; Feng, R.; Hu, T.-L.; Bu, X.-H. Governing metal–organic frameworks towards high stability. *Chem. Com.* **2016**, 52, 8501-8513.
- (18) Mondloch, J. E.; Karagiari, O.; Farha, O. K.; Hupp, J. T. Activation of metal–organic framework materials. *Cryst. Eng. Comm.* **2013**, 15, 9258-9264.
- (19) Murray, L. J.; Dincă, M.; Long, J. R. Hydrogen storage in metal–organic frameworks. *Chem. Soc. Rev.* **2009**, 38, 1294-1314.
- (20) Makal, T. A.; Li, J.-R.; Lua, W.; Zhou, H.-C. Methane storage in advanced porous materials. *Chem. Soc. Rev.* **2012**, 41, 7761-7779.
- (21) Ma, L.; Abney, C.; Lin, W. Enantioselective catalysis with homochiral metal–organic frameworks. *Chem. Soc. Rev.* **2009**, 38, 1248-1256.
- (22) Lee, J.Y. Farha, O. K.; Roberts, J.; Scheidt, K. A.; Nguyena, S.B. T.; Hupp, J. T. Metal–organic framework materials as catalysts. *Chem. Soc. Rev.* **2009**, 38, 1450-1459.
- (23) Keskin, S.; Sholl, D. S. Selecting metal organic frameworks as enabling materials in mixed matrix membranes for high efficiency natural gas purification. *Energy Environ. Sci.* **2010**, 3, 343-351.
- (24) Li, J.-R.; Sculley, J.; Zhou, H.-C. Metal–Organic Frameworks for Separations. *Chem. Rev.* **2012**, 112, 2, 869–932.
- (25) Horike, S.; Umeyama, D.; Kitagawa, S. Ion Conductivity and Transport by Porous Coordination Polymers and Metal–Organic Frameworks. *Acc. Chem. Res.* **2013**, 46, 11, 2376–2384.
- (26) Zhang, X.; Chen, A.; Zhong, M.; Zhang, Z.; Zhang, X.; Zhou, Z.; Bu, X.-H. Metal–Organic Frameworks (MOFs) and MOF-Derived Materials for Energy Storage and Conversion. *Electrochem. Energ. Rev.* **2019**, 2, 29–104.
- (27) Horcajada, P.; Gref, R.; Baati, T.; Allan, P. K.; Maurin, G.; Couvreur, P.; Férey, G.; Morris, R. E.; Serre, C. Metal–Organic Frameworks in Biomedicine. *Chem. Rev.* **2012**, 112, 2, 1232–1268.

- (28) Farha, O. K.; Eryazici, I.; Jeong, N. C.; Hauser, B. G.; Wilmer, C. E.; Sarjeant, A. A.; Snurr, R. Q.; Nguyen, S.B. T.; Yazaydin, A. Ö.; Hupp, J. T. Metal–Organic Framework Materials with Ultrahigh Surface Areas: Is the Sky the Limit? *J. Am. Chem. Soc.* **2012**, 134 (36), 15016-15021.
- (29) Kumar, P.; Anand, B.; Tsang, Y. F.; Kim, K.-H.; Khullar, S.; Wang, B. Regeneration, degradation, and toxicity effect of MOFs: Opportunities and challenges. *Env. Res.* **2019**, 176, 108488.
- (30) Feng, D.; Wang, K.; Wei, Z.; Chen, Y.-P.; Simon, C.M.; Arvapally, R. K.; Martin, R. L.; Bosch, M.; Liu, T.-F.; Fordham, S.; Yuan, D.; Omary, M. A.; Haranczyk, M.; Smit, B.; Zhou, H.-C. Kinetically tuned dimensional augmentation as a versatile synthetic route towards robust metal–organic frameworks. *Nat. Comm.* **2014**, 5, 5723.
- (31) Feng, Y.; Wang, Z.; Fan, W.; Kang, Z.; Feng, S.; Fan, L.; Hu, S.; Sun, D. Engineering the pore environment of metal–organic framework membranes via modification of the secondary building unit for improved gas separation. *J. Mater. Chem. A* **2020**, 8, 13132-13141.
- (32) Belmabkhout, Y. et al. Metal-organic frameworks to satisfy gas upgrading demands: fine-tuning the soc-MOF platform for the operative removal of H<sub>2</sub>S. *J. Mater. Chem. A* **2017**, 5, 3293-3303.
- (33) Han, Y.; Yang, H.; Guo, X. Synthesis Methods and Crystallization of MOFs, *IntechOpen* **2020**.
- (34) Zhang, B.; Zhang, J.; Liu, C.; Sang, X.; Peng, L.; Ma, X.; Wu, T.; Hana, B.; Yanga, G. Solvent determines the formation and properties of metal–organic frameworks. *RSC Adv.* **2015**, 5, 37691-37696.
- (35) Oliva, C. M.; Kharisov, B. I.; Kharissova, O. V.; Serrano, T. E. Synthesis and applications of MOF-derived nanohybrids: A review. *Materials Today: Proceedings* **2021**, 46, 8, 3018-3029.
- (36) Webber, T. E.; Liu, W.-G.; Desai, S. P.; Lu, C. C.; Truhlar, D. G.; Penn, R. L.; Role of a Modulator in the Synthesis of Phase-Pure NU-1000. *ACS App. Mat. & Int.* **2017**, 9 (45), 39342-39346.
- (37) Ali, I.; Asim, M.; Khan, T. A. Low-cost adsorbents for the removal of organic pollutants from wastewater. *J. Env. Man.* **2012**, 113, 170-183.
- (38) Rojas, S.; Horcajada, P.; Metal–Organic Frameworks for the Removal of Emerging Organic Contaminants in Water. *Chem. Rev.* **2020**, 120 (16), 8378-8415.

- (39) Barcelò, D.; Kostianoy, A. G. Emerging Organic Contaminants and human health. *Springer* **2012**, Volume 20.
- (40) Yang, Mihi. A current global view of environmental and occupational cancers, *J. Env. Sci. Hea.* **2011**, 29:3, 223-249.
- (41) Lapworth, D. J.; Baran, N.; Stuart, M. E.; Ward, R. S. Emerging organic contaminants in groundwater: A review of sources, fate and occurrence. *Env. Poll.* **2012**, 163, 287-303.
- (42) Dyson, T. Population and food: global trends and future prospects. *Routledge* **1996**.
- (43) Ibáñez, M.; Gracia-Lor, E.; Bijlsma, L.; Morales, E.; Pastor, L.; Hernández, F. Removal of emerging contaminants in sewage water subjected to advanced oxidation with ozone. *J. Haz. Mat.* **2013**, 260, 389-398.
- (44) Wilhelm, S.; Henneberg, A.; Köhler, H.-R.; Rault, M.; Richter, D.; Scheurer, M.; Suchail, S.; Triebkorn, R. Does wastewater treatment plant upgrading with activated carbon result in an improvement of fish health? *Aq. Tox.* **2017**, 192, 184-197.
- (45) Serna-Galvis, E. A.; Botero-Coy, A. M.; Martínez-Pachón, D.; Moncayo-Lasso, A.; Ibáñez, M.; Hernández, F.; Torres-Palma, R. A.; Degradation of seventeen contaminants of emerging concern in municipal wastewater effluents by sonochemical advanced oxidation processes. *Water Research* **2019**, 154, 349-360.
- (46) Acero, J. L.; Benítez, F. J.; Real, F. J.; Roldán, G.; Rodríguez, E. Chlorination and bromination kinetics of emerging contaminants in aqueous systems. *Chem. Eng. J.* **2013**, 219, 43-50.
- (47) Tran, N. H.; Urase, T.; Ngo, H. H.; Hu, J.; Ong, S. L.; Insight into metabolic and cometabolic activities of autotrophic and heterotrophic microorganisms in the biodegradation of emerging trace organic contaminants. *Bioresource Technology* **2013**, 146, 721-731.
- (48) Klammerth, N.; Miranda, N.; Malato, S.; Agüera, A.; Fernández-Alba, A.R.; Maldonado, M.I.; Coronado, J.M. Degradation of emerging contaminants at low concentrations in MWTPs effluents with mild solar photo-Fenton and TiO<sub>2</sub>. *Cat. Tod.* **2009**, 144, 1-2, 124-130.
- (49) Ateia, M.; Helbling, D. E.; Dichtel, W. R. Best Practices for Evaluating New Materials as Adsorbents for Water Treatment. *ACS Materials Letters* **2020**, 2 (11), 1532-1544.

- (50) McKinstry, C.; Cathcart, R. J.; Cussen, E. J.; Fletcher, A. J.; Patwardhan, S. V.; Sefcik, J. Scalable continuous solvothermal synthesis of metal organic framework (MOF-5) crystals. *Chem. Eng. J.* **2016**, 285, 718-725.
- (51) Wang, S.; Wang, X.; Li, L.; Advincula, R. C. Design, synthesis, and photochemical behavior of poly(benzyl ester) dendrimers with azobenzene groups throughout their architecture, *J. Org. Chem.* **2004**, 69, 9073-9084.
- (52) Chen, Z.; Wang, X.; Cao, R.; Idrees, K. B.; Liu, x.; Wasson, M. C; Farha, O. K. Water-Based Synthesis of a Stable Iron-Based Metal–Organic Framework for Capturing Toxic Gases. *ACS Materials Letters* **2020**, 2 (9), 1129-1134.
- (53) Thommes, M.; Kaneko, K.; Neimark, A. V.; Olivier, J. P.; Rodriguez-Reinoso, F.; Rouquerol, J.; Sing, K. S. W. Physisorption of gases, with special reference to the evaluation of surface area and pore size distribution (IUPAC Technical Report). *Pure and Applied Chemistry* **2015**, 87, 9-10, 1051-1069.
- (54) Lord, H.; Pawliszyn, J. *Microextraction of drugs*, *J. Chrom. A* **2000**, 902(1), 17-63.
- (55) Socas-Rodríguez, B.; Herrera-Herrera, A. V.; Asensio-Ramos, M.; Hernández-Borges, J. Analytical separation science, *Ed. Wiley VCH* **2015**, Chapter 6.
- (56) Taima-Mencera, I.; Rocío-Bautista, P.; Pasán, J.; Ayala, J. H.; Ruiz-Pérez, C.; Afonso, A. M.; Lago, A. B.; Pino, V. Influence of ligand functionalization of UiO-66-based metal-organic frameworks when used as sorbents in dispersive solid-phase analytical microextraction for different aqueous organic pollutants, *Molecules* **2018**, 23(11), 2869.
- (57) Dong, M. W.; Wysocki, J.; Ultraviolet detectors: perspectives, principles, and practices, *LCGC North Am.* **2019**, 37(10), 750-759.
- (58) CCDC deposition numbers: PCN-250(Fe): 1922881. PCN-250(Fe-IM): 1956752.
- (59) Drake, H. F. et al. The thermally induced decarboxylation mechanism of a mixed-oxidation state carboxylate-based iron metal–organic framework, *Chem. Comm.* **2019**, 55, 12769-12772.
- (60) Webb, P. A.; Orr, C. Analytical methods in fine particle technology, *Micrometrics* **1997**.